Appl. Phys. B (2014) 117:245–251
DOI 10.1007/s00340-014-5828-8

Applied Physics B
Lasers and Optics

Single-QCL-based absorption sensor for simultaneous trace-gas detection of CH_4 and N_2O

Wei Ren · Wenzhe Jiang · Frank K. Tittel

Received: 3 March 2014 / Accepted: 27 March 2014 / Published online: 19 April 2014

Abstract A quantum cascade laser (QCL)-based absorption sensor for the simultaneous dual-species monitoring of CH_4 and N_2O was developed using a novel compact multipass gas cell (MGC). This sensor uses a thermoelectrically cooled, continuous wave, distributed feedback QCL operating at ~7.8 μm. The QCL wavelength was scanned over two neighboring CH_4 (1275.04 cm^{-1}) and N_2O (1274.61 cm^{-1}) lines at a 1 Hz repetition rate. Wavelength modulation spectroscopy ($f = 10$ kHz) with second harmonic ($2f$) detection was performed to enhance the signal-to-noise ratio. An ultra-compact MGC (16.9 cm long and a 225 ml sampling volume) was utilized to achieve an effective optical path length of 57.6 m. With such a sensor configuration, a detection limit of 5.9 ppb for CH_4 and 2.6 ppb for N_2O was achieved, respectively, at 1-s averaging time.

1 Introduction

Atmospheric concentrations of greenhouse gases carbon dioxide (CO_2), methane (CH_4) and nitrous oxide (N_2O) now substantially exceed the highest concentrations recorded in ice cores during the past 800,000 years [1, 2]. Compared to CO_2, the warming impact of the most prevalent greenhouse gases, CH_4 and N_2O, is 25 and 300 times greater during a 100-year period. Wetlands and human activities such as leakage from natural gas systems and the raising of livestock are the major CH_4 emission sources. N_2O is produced mainly by microbial processes in soil and water or human activities such as agriculture, fossil fuel combustion, wastewater management and industrial processes. Reliable and sensitive detection of atmospheric CH_4 and N_2O is crucial to environmental considerations, as these measurements can be used to determine CH_4/N_2O sources, leading to an improved understanding of climate change [2].

Atmospheric detection of CH_4 and N_2O concentration levels using laser-based gas sensors has been reported by numerous research groups in recent years [3–8]. A compact mid-infrared absorption spectrometer for N_2O and CH_4 was developed using thermoelectrically cooled (TEC), pulsed quantum cascade lasers (QCLs) and a multipass gas cell (MGC) with 56 m path length and 0.5 l volume [3]. High-precision simultaneous measurements of N_2O (3 ppb) and CH_4 (7 ppb) near 7.9 μm were achieved at a pressure of 60 torr and 1-s averaging time. An open-path ambient CH_4 and N_2O sensor system based on a pulsed distributed feedback (DFB) QCL near 7.7 μm and a 215 m path length MGC was reported in Ref. [4]. A minimum detection limit of 2 and 7 ppb was achieved for N_2O and CH_4 at atmospheric pressure, respectively, by detecting the N_2O absorption line at 1299.38 cm^{-1} and CH_4 lines at 1299.62 and 1299.90 cm^{-1}. Simultaneous detection of atmospheric N_2O and CO was recently described using a continuous wave (cw) 4.5 μm QCL combined with a portable open-path MGC (16 m effective length, atmospheric pressure) to provide a precision of 0.15 ppb N_2O at 10 Hz [5]. A QCL-based absorption spectrometer (QCLAS) was developed for in situ measurements of atmospheric N_2O and CH_4 emission fluxes by implementing multiple QCLs near 4.5, 7.4 and 7.9 μm to obtain different detection sensitivities [6]. This QCLAS system with an absorption path length of 76 m, an operating temperature of 300 K, and a pressure of 50 mbar was employed in a field campaign to investigate the impact of

W. Ren (✉) · W. Jiang · F. K. Tittel
Department of Electrical and Computer Engineering, Rice University, 6100 Main Street, Houston, TX 77005, USA
e-mail: wr5@rice.edu

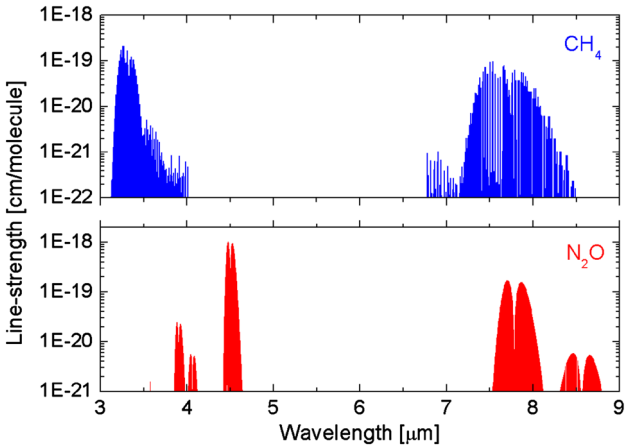

Fig. 1 Mid-infrared absorption line-strengths of CH_4 and N_2O at 296 K (HITRAN database [9])

environmental intensive pig farming. Cavity-enhanced absorption spectroscopy (CEAS) achieved a minimum detection limit of 10 ppb at a pressure of 30 torr when targeting a N_2O absorption line at 4.53 μm [7]. In this technique, two pairs of mirrors with high-reflectivity (>99.9 %) as well as critical optical alignment were required to achieve optimal performance of the CEAS-based sensor system. More recently, a quartz-enhanced photoacoustic spectroscopy (QEPAS)-based CH_4 and N_2O sensor was developed for environmental and biomedical measurements [8]. Detection limits of 13 ppb for CH_4 at 1275.04 cm^{-1} and 6 ppb for N_2O at 1275.49 cm^{-1} were achieved at a 1-s data acquisition time using a cw DFB-QCL.

CH_4 and N_2O have absorption spectra in the mid-infrared region as illustrated in Fig. 1, where the absorption line-strengths are plotted as a function of wavelength from 3 to 9 μm [9]. The spectral plot shown in Fig. 1 reveals that the strongest absorption band for CH_4 is located at 3.3 μm and for N_2O at 4.5 μm, respectively. Furthermore, these two gas molecules have strong spectral overlap in the wavelength range between 7.5 and 8 μm, corresponding to the v_1 fundamental band of CH_4 and v_4 fundamental band of N_2O, respectively. An appropriate choice of detection wavelengths enables the possibility of simultaneous measurements of multi-species using a single laser, greatly simplifying the sensor system and reducing its cost.

In this paper, we report the development of a trace-gas sensor for the simultaneous dual-species monitoring of atmospheric CH_4 and N_2O using a single 7.8 μm DFB-QCL. Two neighboring CH_4 (1275.04 cm^{-1}) and N_2O (1274.61 cm^{-1}) absorption lines can be acquired using a single QCL wavelength scan. An ultra-compact MGC (16.9 cm long, 225 ml volume) was utilized to achieve an effective optical path length of 57.6 m. Details of sensor configuration, calibration and long-term stability are described in this work. This absorption sensor system provides a compact, reliable and precise diagnostic strategy for atmospheric CH_4 (~1.80 ppm [1]) and N_2O (~320 ppb [1]) monitoring.

2 Theory and line selection

Laser-based absorption spectroscopy is chosen for many optical trace-gas sensors in a wide variety of applications due to its fast time response and quantitative nature. In particular, wavelength modulation spectroscopy with second harmonic detection (WMS-2*f*) is an extension of direct absorption spectroscopy that has been used extensively for sensitive trace-gas detection. The fundamental theory of laser-based absorption spectroscopy is well understood and only described briefly to clarify the notation and units used in this paper.

2.1 Absorption spectroscopy fundamentals

When laser radiation at a wavelength v passes through a uniform gas medium, the wavelength-dependent transmission τ_v is determined by Beer's law:

$$\tau_v = \left(\frac{I_t}{I_0}\right)_v = \exp\left(-SPx\phi_v L\right), \tag{1}$$

where I_0 and I_t are incident and transmitted radiation intensity, respectively; $S(cm^{-2}\ atm^{-1})$ is the line-strength of the specific transition, P(atm) is the total gas pressure, x is the mole fraction of the absorbing species, ϕ_v(cm) is the line-shape function, and L(cm) is the optical path length. The line-shape function ϕ_v is usually approximated using a Voigt profile characterized by the collision-broadened full-width at half maximum (FWHM) and Doppler broadening FWHM. The dimensionless product:

$$\alpha_v = -\ln\left(\frac{I_t}{I_0}\right)_v = SPx\phi_v L, \tag{2}$$

is known as absorbance, with $k_v = SPx\phi_v$, the absorption coefficient.

In WMS absorption measurements, the laser injection current is sinusoidally modulated at a frequency f to produce simultaneous modulation of the laser wavelength $v(t)$ and intensity $I_0(t)$,

$$v(t) = \bar{v}_0 + a\ \cos\left(2\pi f\right), \tag{3}$$

$$I_0(t) = \bar{I}_0\left[1 + \sum_{n=1}^{\infty} i_n\ \cos\left(n \cdot 2\pi f t + \psi_n\right)\right], \tag{4}$$

where $\bar{v}_0(cm^{-1})$ is the center laser wavelength, $a(cm^{-1})$ is the modulation depth, i_n is the nth Fourier coefficient normalized by the average laser intensity $\bar{I}_0$, and ψ_n is the

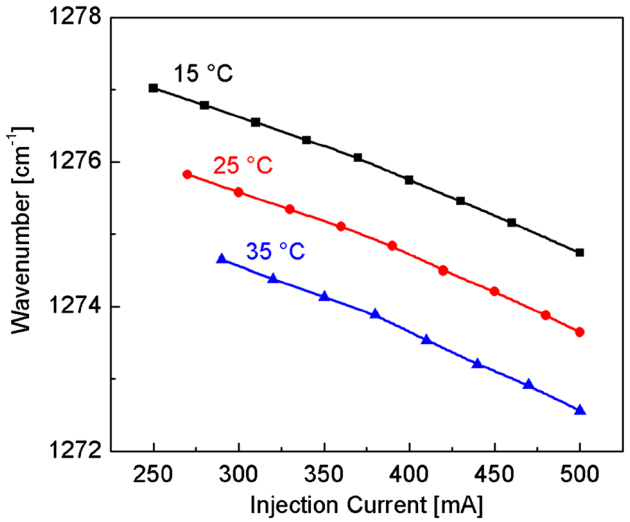

Fig. 2 QCL wavelength performance as a function of injection current at different operating temperatures

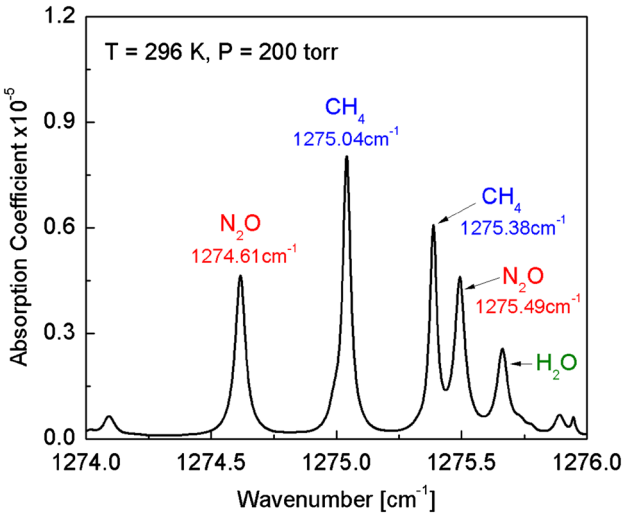

Fig. 3 Simulated absorption spectra of standard air at 296 K and 200 torr using the HITRAN database [9]

phase shift between the wavelength modulation and the nth order intensity modulation.

The transmission coefficient τ_v is also a periodic function that can be expanded in terms of its Fourier series:

$$\tau(t) = \sum_{n=0}^{\infty} H_n \cos(n \cdot 2\pi f t), \quad (5)$$

with H_n the nth order Fourier component as discussed in references [10, 11]. The case of $n = 2$ is generally of the highest interest in WMS, since the second harmonic signal ($2f$) is closely related to the absorption and background free [11]. The $2f$ signal can be experimentally acquired using a lock-in amplifier. The lock-in amplifier functions by multiplying the detector signal with the reference sinusoid at $2f$ and shifting the harmonic component to DC. A low-pass filter is then applied to isolate the DC value and eliminate all other components such as laser and electronic noise outside the filter bandwidth. Hence, WMS-$2f$ detection significantly improves the signal-to-noise ratio (SNR) for small absorption signals. The gas concentration can be inferred from the measured WMS-$2f$ signal provided that the gas temperature, pressure and optical path length are fixed.

2.2 Line selection

Two adjacent CH_4 and N_2O lines need to be selected for simultaneous dual-species measurements within a single QCL scan. These two species have strong overlap in their mid-infrared spectra between 7.5 and 8 μm as shown in Fig. 1 that can be accessed by a commercially available 7.8 μm cw QCL.

The QCL current and temperature tuning characteristics were determined using a Fourier transform infrared (FTIR) spectrometer with a resolution of 0.125 cm^{-1}. Figure 2 demonstrates the wavelength tuning performance of the selected TEC cw DFB-QCL (AdTech Optics). This QCL covers a wavelength range of 1272.2–1277.0 cm^{-1} and the current and temperature tuning coefficients are determined to be −0.01 cm^{-1}/mA and −0.11 cm^{-1}/ °C, respectively.

Absorption spectra based on the HITRAN database [9] are computed for the standard air (1.86 % H_2O, 0.03 % CO_2, 320 ppb N_2O, 1.68 ppm CH_4, 150 ppb CO, 30 ppb O_3, 20.7 % O_2 and 77.4 % N_2), to identify the optimum CH_4 and N_2O transitions. The line pair of the CH_4 transition at 1275.04 cm^{-1} and the N_2O transition at 1274.61 cm^{-1} was selected as depicted in Fig. 3 for the sensor design. These two lines with a line spacing of 0.4 cm^{-1} can be fully swept across by a single QCL wavelength scan (laser temperature at 25 °C, injection current scan between 320 and 420 mA) at a 1 Hz repetition rate. The spectral interference between these two adjacent lines is eliminated by choosing a relatively low pressure. Interfering absorption from other gas molecules present in air was not observed.

3 Experimental details

3.1 Sensor system architecture

Single-laser multi-species sensing design has the advantage of simplifying the sensor system and reducing its cost. The

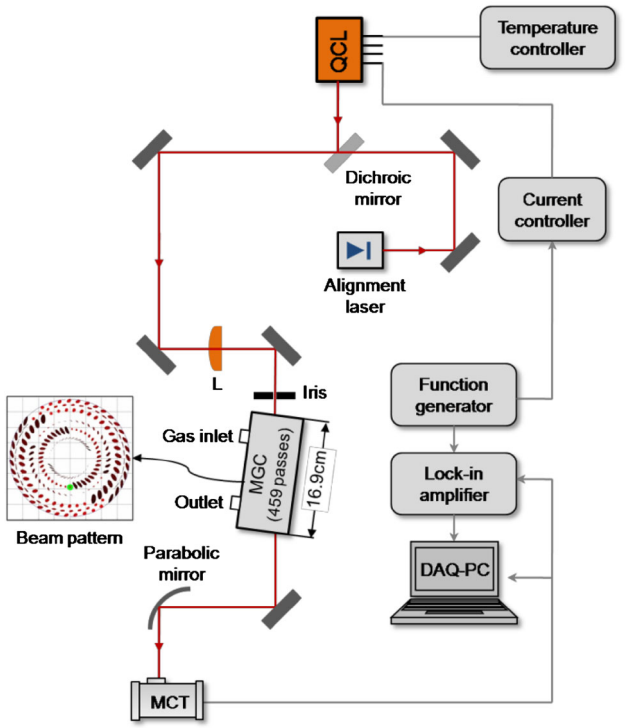

Fig. 4 Schematic of experimental CH_4/N_2O sensor system

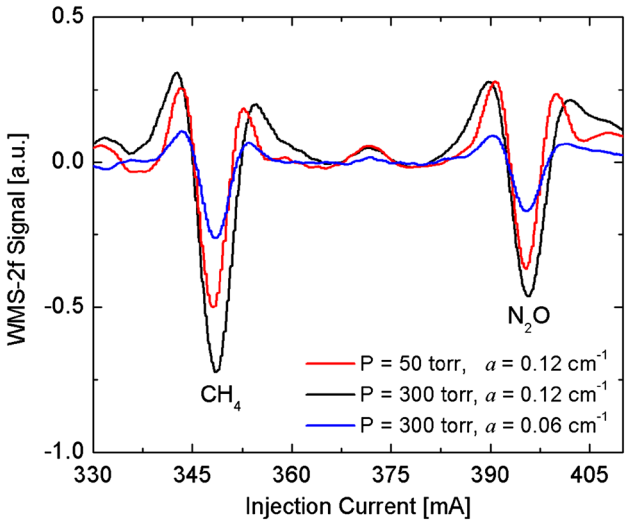

Fig. 5 Measured WMS-2*f* signal of laboratory room air varied with pressure and modulation depth *a*; $T = 296$ K, $L = 57.6$ m

experimental setup for the single-laser-based sensor is schematically depicted in Fig. 4. A TEC cw DFB-QCL (AdTech Optics) with collimation optics in a standard high heat load (HHL) package was used as the monochromatic light source. This QCL was recently used for CH_4 and N_2O detection using QEPAS [8, 12]. The QCL current and temperature were controlled by a commercial current source (ILX Lightwave, LDX-3232) and a temperature controller (Wavelength Electronics, MPT10000), respectively. A visible diode laser beam ($\lambda = 630$ nm) was combined with the mid-infrared beam by means of a dichroic mirror (ISP Optics, model BSP-DI-25-3) to assist in the optical alignment of the sensor system.

Both visible and infrared laser beams were directed into a novel MGC (Sentinel Photonics) with a 57.6 m effective path length using a ZnSb lens (200 mm focus length). This dense patterned MGC consists of two spherical mirrors (diameter 40 mm) separated by a distance of 12.5 cm, providing a total cell length of 16.9 cm and a sampling volume of 225 ml. The spot pattern created in this new MGC covers more of the mirror surface (see spot pattern in Fig. 4) compared to a standard Herriott cell with a simple circle or elliptical pattern. More than 450 beam passes are made with minimized spot overlap, hence reducing etalon fringe effects. The pressure inside the MGC is managed by using a pressure controller (MKS, type 649) and a diaphragm vacuum pump (KNF, type UN816.3 KTP). Further details of the MGC configuration can be found in Ref. [13], where a similar MGC was used for trace-gas detection of ethane at 3.36 μm.

In this study, the output infrared laser beam was focused onto a liquid nitrogen cooled mercury cadmium telluride (MCT) detector, followed by WMS-2*f* detection for sensitive trace-gas measurements. A superposition of a 1 Hz voltage ramp and 10 kHz sinusoidal dither provided by a function generator (Tektronix AFG 3022B) was applied to the QCL current driver to scan and modulate the laser frequency across the CH_4/N_2O absorption features. The signal from MCT detector was first amplified with a current pre-amplifier and further processed by a lock-in amplifier (Signal Recovery 7265 DSP) to extract its 2*f* signal. The processed data were subsequently collected using a DAQ card (NI-DAQ-AI-16XE-50, National Instrument) and displayed by a PC via a LabVIEW interface.

3.2 Optimization for simultaneous detection

The WMS-2*f* peak height is dependent on the line shape related to gas pressure and the wavelength modulation depth *a* [10]. Figure 5 depicts three typical room-temperature WMS-2*f* signals of CH_4 and N_2O in laboratory air with different pressures and modulation depth values, indicating that an appropriate choice of these parameters was required to optimize the detection sensitivity of the sensor system.

The WMS-2*f* amplitudes of CH_4 and N_2O measured at different pressures and modulation depths are plotted in Fig. 6 for comparison. These measurements were conducted by laboratory air flowed through the MGC with

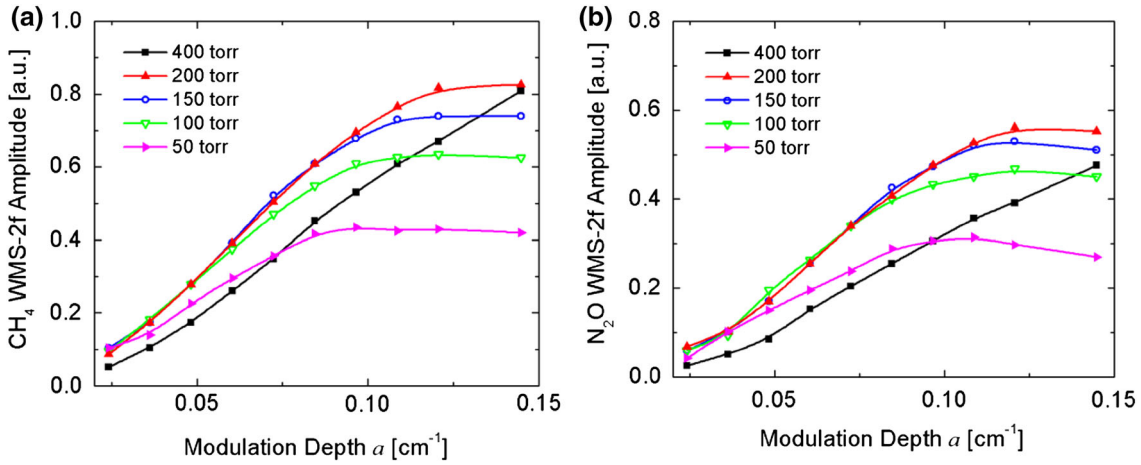

Fig. 6 Measured WMS-2*f* signal amplitude as a function of the laser modulation depth at different pressures for **a** CH_4 and **b** N_2O in laboratory room air

pressure for each test maintained by the pressure controller. The gas pressure was controlled to below 400 torr in order to eliminate possible cross-talk absorption interference between these two neighboring CH_4 and N_2O lines. According to the experimental results shown in Fig. 6, with the choice of pressure of ~200 torr and a modulation depth near 0.12 cm^{-1}, both CH_4 and N_2O were found to reach the maximum WMS-2*f* amplitudes. Hence, these parameters were selected in this study for the sensor development.

In the current experimental setup, the optical path outside the MGC was open to air and estimated to have a length of ~40 cm. The N_2O and CH_4 absorption in the ambient air is 140 times weaker compared to the gas absorption inside the MGC with a path length of 57.6 m. Additionally, the wavelength modulation depth was optimized for a MGC pressure of 200 torr, and thus the interference of N_2O and CH_4 in the ambient air with relatively broader absorption spectra was negligible. In fact, the whole system can be purged with nitrogen in a field measurement if there is significant difference in N_2O and CH_4 concentrations between the sample gas and the ambient air.

4 Measurements and results

4.1 Sensor calibration

The sensor calibration was performed using the experimental setup depicted in Fig. 4 with optimized pressure and selected modulation depth values. Two certified gas cylinders (Matheson Inc.) of 5.4 ppm CH_4:N_2 and 2.1 ppm N_2O:N_2 supplied different mixing ratios using a commercial gas dilution system (Environics, Series 4040).

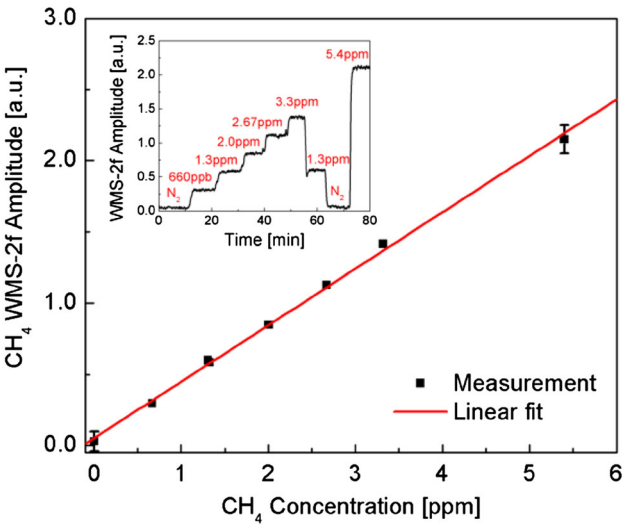

Fig. 7 WMS-2*f* amplitude at 1275.04 cm^{-1} as a function of CH_4 concentration (linear fit equation: $y = 0.054 + 0.396x$). Inset: continuous monitoring of WMS-2*f* amplitude for 1.5 h with time-varying CH_4 concentration levels

In this calibration process, the WMS-2*f* amplitude was recorded for ~10 min for each calibrated concentration of the test gas. The measured WMS-2*f* amplitude at 1275.04 cm^{-1} is plotted in Fig. 7 as a function of the CH_4 concentration. The CH_4 concentration covers a range from 660 ppb to 5.4 ppm to demonstrate the linear response of the sensor system. The coefficient of determination (R squared value) for linear fitting is >0.99 and the relative difference between the calibrated and the measured CH_4 concentration based on the determined linear equation is within 7 % (actually <4 % when CH_4 concentration is higher than 660 ppb). The WMS-2*f* amplitude remains

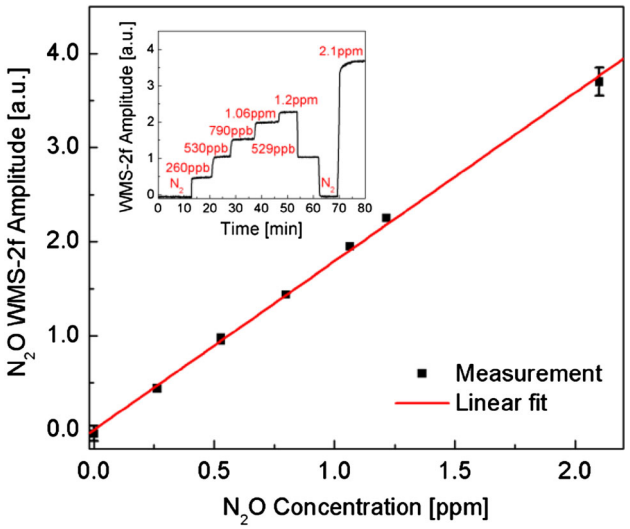

Fig. 8 WMS-2*f* amplitude at 1274.61 cm^{-1} as a function of N_2O concentration (linear fit equation: $y = 0.003 + 1.791x$). Inset: continuous monitoring of WMS-2*f* amplitude for 1.5 h with time-varying N_2O concentration levels

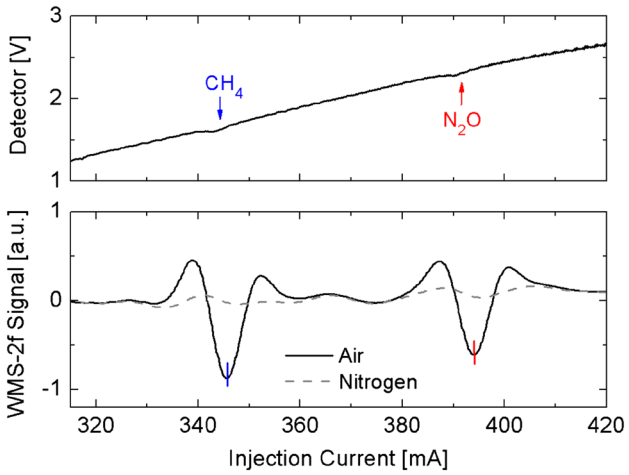

Fig. 9 Recorded detector signal (*top panel*, direct absorption without sinusoidal modulation) and WMS-2*f* signal (*bottom panel*) for ambient air at a pressure of 200 torr and a modulation depth of 0.12 cm^{-1}

stable for different CH_4 concentrations and the sensor reproducibility was tested by detecting 1.3 ppm CH_4 after 55 min of continuous measurements as illustrated by the inset graph in Fig. 7.

A similar sensor calibration was performed for N_2O detection at 1274.61 cm^{-1} using the same laser wavelength scan as that for CH_4 detection. The linear response of the sensor system was plotted in Fig. 8 for different N_2O concentrations ranging from 260 ppb to 2.1 ppm. The *R* squared value for linear fitting is >0.99 and the sensor reproducibility was tested by measuring 530 ppb N_2O after 55 min of continuous monitoring. All these measurements indicate that this single-QCL-based absorption sensor is capable of the simultaneous detection of CH_4 and N_2O in air with high sensitivity and stability.

4.2 Sensor performance

Continuous monitoring of CH_4 and N_2O in laboratory room air was performed to examine the sensor performance. Figure 9 depicts a representative sweep of both absorption lines at a pressure of 200 torr. The sweep is $\sim$0.8 cm^{-1} wide and acquired in 1 s while monitoring ambient air. The concentrations determined from the WMS-2*f* amplitudes in Fig. 9 (1.83 ppm for CH_4 and 335 ppb for N_2O) show very good agreement with typical ambient values (1.80 ppm for CH_4 and 324 ppb for N_2O [1]).

The long-term stability and precision of the CH_4/N_2O sensor were tested by monitoring the laboratory air for 1.5 h. Figure 10a and b present the 1 Hz raw data time series of CH_4 and N_2O concentration, respectively. The root mean square (RMS) noise during the entire period is 5.9 ppb (or $\sim$0.3 % of the ambient level) for CH_4 and 2.6 ppb (or $\sim$0.8 % of the ambient level) for N_2O. Considering the absorption line-strengths of these two molecules (HITRAN database [9]), a gas pressure of 200 torr, and optical path length of 57.6 m, a minimum detection absorption coefficient of 2.5×10^{-8} cm^{-1} was achieved for both molecules using the current sensor configuration. An Allan deviation [14] plot for the 1.5-h period sampling room air is shown in Fig. 10c. The stability of the sensor system in a free running, non-wavelength locked mode allows averaging of up to 200 s for the detection of both CH_4 and N_2O. The minimum of the Allan deviation corresponds to <1.4 ppb for CH_4 and <0.3 ppb for N_2O for an averaging time of 200 s.

Finally, it is of interest to investigate the factors limiting the sensitivity of the current sensor system. These tests were performed by flowing pure nitrogen through the MGC and monitoring the lock-in amplifier output at the target laser wavelength at 1-s averaging time. Here, the CH_4 absorption line at 1275.04 cm^{-1} was used as an example. In most absorption spectroscopy measurements, the major noise sources include detector noise, laser beam noise and optical fringe noise. First of all, the detector noise is not a significant contributor in our system. With the laser beam blocked, the detector sensitivity was measured to be only 0.3 ppb for CH_4, which is almost 20 times lower compared to the CH_4 system sensitivity of 5.9 ppb. Secondly, the laser beam noise can be measured by removing the modulation voltage from the QCL current driver but allowing the laser beam to be incident on the detector. The 10 kHz sinusoid from the function generator was used as reference signal by the lock-in amplifier for 2*f* detection. The beam noise level was measured to be $\sim$3 ppb, which is considered as the major sensitivity limiting factor. The optical

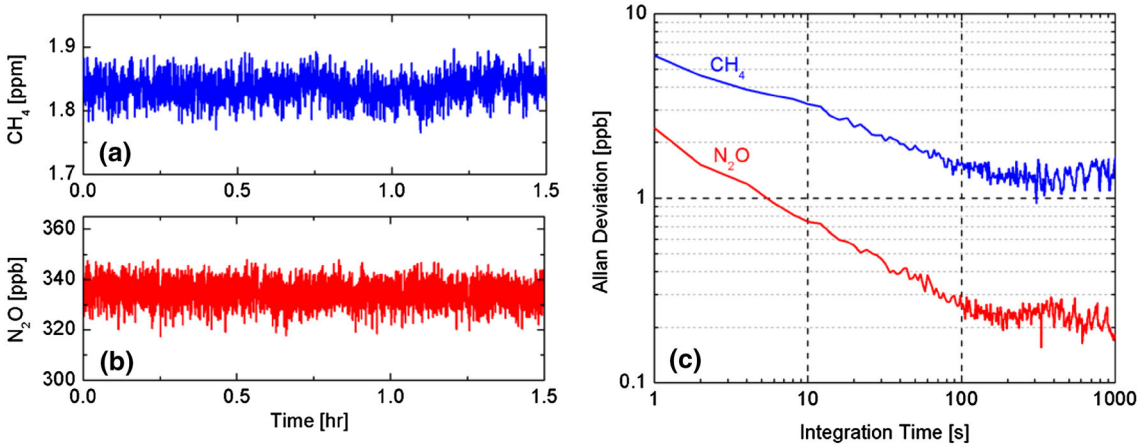

Fig. 10 Simultaneous monitoring of **a** CH_4 and **b** N_2O in laboratory air for 1.5 h. **c** Allan deviation in ppb of the CH_4 and N_2O concentrations as a function of integration time

fringe noise, which is the third noise source present during CH_4 detection, is thus two times larger than the beam noise. Therefore, the primary limiting factor of the detection sensitivity in the current sensor setup is the optical fringe noise, which can be reduced by optimizing the optical alignment. However, the sensitivity can only be improved by a maximum factor of two due to the remaining system noise caused by random amplitude noise present on the QCL beam.

5 Conclusions

We have demonstrated the development of a single-QCL-based absorption sensor for the simultaneous detection of atmospheric CH_4 and N_2O at $\sim$7.8 μm using a novel compact MGC. Two neighboring CH_4 (1275.04 cm^{-1}) and N_2O (1274.61 cm^{-1}) absorption lines can be swept by a single laser wavelength scan at a 1 Hz repetition rate. Such a sensor configuration has the advantage of significantly reducing the cost and simplifying the sensor system. WMS with second harmonic detection was conducted to achieve ppb-level detectivity of both gas molecules at 1-s averaging time. The sensor calibration was performed using commercially available, certificated gas cylinders. The long-term stability and precision of this CH_4/N_2O sensor were examined by monitoring the laboratory room air for 1.5 h and a sub-ppb detectivity can be achieved by averaging up to 200 s. The primary limiting factors of the detection sensitivity in the current sensor system were determined to be the QCL beam noise and optical fringe noise. Future work is planned by installing the sensor system in a mobile monitoring van for real time measurements of CH_4 and N_2O emissions in the Greater Houston area.

Acknowledgments The authors gratefully acknowledge the financial support from a National Science Foundation (NSF) ERC MIR-THE award, a NSF-ANR award for international collaboration in chemistry, "Next generation of Compact Infrared Laser based Sensor for Environmental Monitoring (NexCILAS)" and the Robert Welch Foundation Grant C-0586.

References

1. IPCC, Climate Change, *The Physical Science Basis Intergovernmental Panel on Climate Change* (Cambridge University Press, Cambridge, 2013)
2. S.A. Montzka, E.J. Dlugokencky, J.H. Butler, Nature **476**, 43 (2011)
3. D.D. Nelson, B. McManus, S. Urbanski, S. Herndon, M.S. Zahniser, Spectrochim. Acta. A. Mol. Biomol. Spectrosc. **60**, 3325 (2004)
4. P.C. Castillo, I. Sydoryk, B. Gross, F. Moshary, Proc. SPIE **8718**, 87180J (2013)
5. L. Tao, K. Sun, M.A. Khan, D.J. Miller, M.A. Zondlo, Opt. Express **20**, 28106 (2012)
6. I. Mappé, L. Joly, G. Durry, X. Thomas, T. Decarpenterie, J. Cousin, N. Dumelie, E. Roth, A. Chakir, P.G. Grillon, Rev. Sci. Instrum. **84**, 023103 (2013)
7. J. Wojtas, Z. Bielecki, T. Stacewicz, J. Mikolajczyk, R. Medrzycki, B. Rutecka, Acta Phys. Pol. A **120**, 794 (2011)
8. M. Jahjah, W. Ren, P. Stefański, R. Lewicki, J. Zhang, W. Jiang, J. Tarka, F.K. Tittel, Analyst **139**, 2065 (2014)
9. L.S. Rothman, I.E. Gordon, A. Barbe, D.C. Benner, P.F. Bernath, M. Birk, V. Boudon, L.R. Brown, A. Campargue, J.-P. Champion et al., J. Quant. Spectrosc. Radiat. Transf. **110**, 533 (2009)
10. P. Kluczynski, O. Axner, Appl. Opt. **38**, 5803 (1999)
11. H. Li, G.B. Rieker, X. Liu, J.B. Jeffries, R.K. Hanson, Appl. Opt. **45**, 1052 (2006)
12. M. Jahjah, W. Jiang, N.P. Sanchez, W. Ren, P. Patimisco, V. Spagnolo, S.C. Herndon, R.J. Griffin, F.K. Tittel, Opt. Lett. **39**, 957 (2014)
13. K. Krzempek, M. Jahjah, R. Lewicki, P. Stefański, S. So, D. Thomazy, F.K. Tittel, Appl. Phys. B **112**, 461 (2013)
14. P. Werle, R. Mücke, F. Slemr, Appl. Phys. B **57**, 131 (1993)